RSC Advances

Photocatalytic water oxidation over PbCrO$_4$ with 2.3 eV band gap in IO$_3^-$/I$^-$ redox mediator under visible light

SCHOLARONE™
Manuscripts

RSC Advances

COMMUNICATION

Photocatalytic water oxidation over PbCrO$_4$ with 2.3 eV band gap in IO$_3^-$/I$^-$ redox mediator under visible light

Y. Miseki*, O. Kitao, and K. Sayama*

PbCrO$_4$ was prepared by a simple precipitation method under ambient conditions; its band gap was estimated to be 2.3 eV. Pt-loaded PbCrO$_4$ exhibited high photocatalytic activity in aqueous NaIO$_3$, promoting water oxidation to generate O$_2$. Photonic efficiency (apparent quantum yield) at 420 nm was estimated to be 1.0 %.

Various solar energy conversion systems that convert solar energy to chemical fuels, such as hydrogen, have gained increasing attention. For example, the two-photon excitation system (Z-scheme system), which employs two powdered photocatalysts and a suitable redox mediator, and the photocatalysis-electrolysis hybrid system have been widely studied as solar energy conversion systems because the evolved H$_2$ and O$_2$ products are separable.[1-5] Since the photocatalyzed oxidation of water to O$_2$ is a four-electron transfer process, it is an essential and challenging step. The stability of metal oxide semiconductors makes them attractive candidates as photocatalysts for water oxidation. However, most metal oxide photocatalysts are unavailable for visible light due to their wide band gaps (BG); these are derived from the deep (positive) valence bands, which consist of the O2p orbital. It has been reported that metal oxide complexes such as PbMoO$_4$ (BG: 3.3 eV),[6] RbPb$_2$Nb$_3$O$_{10}$ (BG: 2.6 eV),[7] Bi$_2$WO$_6$ (BG: 2.8 eV),[8] BiVO$_4$ (BG: 2.4 eV),[9] AgNbO$_3$ (BG: 2.9 eV),[10] PbBi$_2$Nb$_2$O$_9$ (BG: 2.9 eV),[11] and SnNb$_2$O$_6$ (BG: 2.3 eV),[12] which contain Bi^{3+}, Pb^{2+}, Sn^{2+}, and Ag$^+$ cations, possess shallower (more negative) valence bands due to s-p orbital hybridization. Therefore, these oxides have received great attention for their use in designing visible light-induced photocatalysts. An oxide of interest is PbCrO$_4$, which is a water-insoluble orange pigment that exhibits favorable optical absorption properties,[13] and is obtained as single crystal nanorods via a simple precipitation method.[14] In this study, we observed water oxidation in the presence of IO$_3^-$/I$^-$ as a reversible redox mediator under visible light (up to 550 nm) over a Pt/PbCrO$_4$ photocatalyst possessed the smallest BG (2.3 eV) compared to other oxide semiconductor photocatalysts with s-p hybrid orbital in valence band. Additionally, we elucidated the band structure of PbCrO$_4$ via diffuse reflection spectroscopy, valence band X-ray photoelectron spectroscopy, Mott-Schottky plots, and density functional theory calculations.

PbCrO$_4$ powder was prepared by a simple precipitation method under ambient conditions. Pb(NO$_3$)$_3$ (Wako Pure Chemical; 99.5+%) and (NH$_4$)$_2$CrO$_4$ (Kanto Chemical; 97%) were employed as starting materials. Individual solutions of each metal compound (1.6 mmol) in distilled water (200 mL) were mixed at ambient conditions to immediately afford a yellow precipitate. After the suspension was aged for 1 h (rotating speed: 900 rpm), the precipitate was filtered, washed, and dried at 343 K for 2 h. A Pt cocatalyst was loaded onto the PbCrO$_4$ powder via photodeposition, impregnation, and chemical reduction methods. In the latter method, the PbCrO$_4$ powder (0.2 g) and a H$_2$PtCl$_6$ (30.8 μmol, Wako Pure Chemical; 98.5+%) were dispersed in ethanol (40 mL), and then heated in an oil bath at 373 K for 1 h. The resulting powder was filtered, washed, and dried at 343 K for 2 h. Additional thermal treatment in air at 473 K was conducted to improve the contact between the Pt cocatalyst and the PbCrO$_4$ photocatalyst. The preparation conditions about impregnation and photodeposition methods were shown in ESI. To prepare the PbCrO$_4$ electrode, the PbCrO$_4$ powder was coated on an F-doped SnO$_2$ (FTO) conductive glass substrate (surface resistance 10 Ω/sq, Nippon Sheet Glass Co., Ltd.) by the squeegee method. The squeegee method is often used to fix a photocatalyst powder onto a conductive substrate for preparing photoelectrodes. Slurry was prepared by mixing 20 mg of PbCrO$_4$ with 200 μL of distilled water, and then was spread onto a conductive glass plate with a glass rod and heated in air at 573 K for 1 h. The phase purity of the resulting powder was confirmed by X-ray diffraction studies (PANalytical, EMPYREAN). The surface condition and valence band information were analyzed using an X-ray photoelectron spectrometer (Ulvac-Phi, XPS-1800). Photocatalytic reactions were performed in a side-window cell made of Pyrex connected to a gas-closed circulation system. A 300-W Xe illuminator (ILC Technology, Inc., CERMAX-LX300) was attached to cut-off filters (HOYA Corporation) and employed for visible light irradiation experiments. Using a magnetic stirrer, the photocatalyst powder (10–150 mg) was dispersed in an aqueous solution (300 mL) of either 20 mM AgNO$_3$ or 2 mM NaIO$_3$. The amount of O$_2$ evolved was determined via on-line gas chromatography (Shimadzu Corporation, MS-5A column, TCD, Ar carrier). The amount of I$^-$ ions produced was determined by a color reaction between I$^-$ and IO$_3^-$ ions under acidic conditions, from which I$_3^-$ was generated. Photonic efficiency (apparent quantum yield) was evaluated using a 420 nm monochromatic light (7.6

mWcm^2, 1.6 ×10^{16} photon s^{-1}) as a light source. The number of incident photons was determined using a Si photodiode that was proofread by NMIJ (National Metrology Institute of Japan).

It was confirmed that monoclinic phase of PbCrO$_4$ possessing crocoite structure successfully prepared by simple precipitation method via X-ray diffraction pattern, and PbCrO$_4$ particles have attractive optical absorption property (BG: 2.3 eV, Figure 1 inserted) and have single crystal like nanorod shape via measuring scanning electron microscopy (SEM) image (Figure S1). Table 1 shows the O$_2$ evolution rates with PbCrO$_4$ powder in the presence of Ag$^+$ or IO$_3^-$ ions under visible light. Pristine PbCrO$_4$ powder facilitated O$_2$ evolution in aqueous AgNO$_3$ solution, but not in aqueous NaIO$_3$ solution. This result indicates that native PbCrO$_4$ powder lacks the sites on which IO$_3^-$ reduction can occur. Therefore, we introduced a Pt cocatalyst onto PbCrO$_4$ particles using various loading methods. As a result, relatively high rates of O$_2$ evolution were observed only in the presence of Pt/PbCrO$_4$, which was prepared by a chemical reduction method in the liquid phase. Optimal amount of Pt loaded was 3 wt% for PbCrO$_4$. We confirmed that no O$_2$ evolution took place in absence of light or redox oxidants (Ag$^+$ or IO$_3^-$). The X-ray photoelectron spectra of Pt4f$_{7/2}$ on Pt/PbCrO$_4$ powders revealed that the Pt cocatalyst possesses different valences depending on the loading method employed; Pt was loaded as Pt^0 metal using the chemical reduction method, while Pt was loaded as PtO$_x$ using the impregnation and photodeposition methods (Figure S2). Overall, Pt metal was observed as an efficient cocatalyst in aqueous NaIO$_3$ solution for photocatalyzed O$_2$ evolution reactions.

Figure 1 illustrates the dependence of the O$_2$ evolution rate on

Table 1 Photocatalytic O$_2$ evolution rates of PbCrO$_4$ powders in the presence of Ag$^+$ or IO$_3^-$ ions under visible light[a]

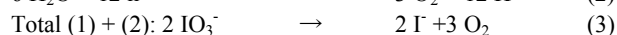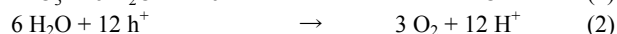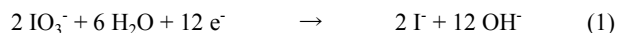| Photocatalyst	Loading method	O$_2$ evolution rates / μmol h^{-1}	
		(AgNO$_3$)	(NaIO$_3$)
PbCrO$_4$	-	26	0
Pt/PbCrO$_4$[b]	Chemical reduction	58	13
Pt/PbCrO$_4$[b]	Impregnation	12	1
Pt/PbCrO$_4$[b]	Photodeposition	7	0

[a]Catalyst: 50 mg, reactant solution: 300 mL, light source: 300 W Xe arc lamp attached with L42 cut off filter. [b]Amount of Pt loaded: 3 wt%.
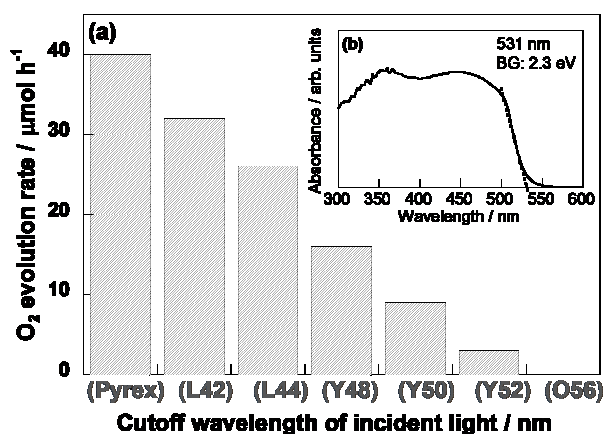
Figure 1 (a) Dependence of the initial O$_2$ evolution rate of Pt-loaded PbCrO$_4$ on the cut-off wavelength of the incident light. Catalyst (150 mg), reactant solution (300 mL), light source (300 W Xe arc lamp attached with cut-off filters). Amount of Pt loaded: 3 wt%. (b) Diffuse reflection spectrum of PbCrO$_4$

the cut-off wavelength of the incident light. Photocatalyzed O$_2$ evolution from aqueous NaIO$_3$ solution was observed even when the cut-off wavelength was 520 nm (3 μmol h^{-1}), and the O$_2$ evolution rate decreased as the cut-off wavelength increased. We thus concluded that water oxidation proceeded via band gap transitions (2.3 eV = 550 nm threshold wavelength) for the PbCrO$_4$ photocatalyst. The photonic efficiency under monochromatic light at 420 nm was estimated to be ca. 1 %.

Figure 2 shows the time course of photocatalyzed O$_2$ evolution over 10 mg of Pt(3 wt%)/PbCrO$_4$ in an aqueous NaIO$_3$ solution. The turnover numbers of the reacted electrons/holes with respect to the molar quantities of Pt and PbCrO$_4$ reached 115 and 5.5, respectively. O$_2$ and I$^-$ are produced according to the equations below in the photocatalyzed water oxidation reactions in the presence of IO$_3^-$ ion.

$$2\ IO_3^- + 6\ H_2O + 12\ e^- \quad \rightarrow \quad 2\ I^- + 12\ OH^- \quad (1)$$
$$6\ H_2O + 12\ h^+ \quad \rightarrow \quad 3\ O_2 + 12\ H^+ \quad (2)$$
$$\text{Total (1) + (2): } 2\ IO_3^- \quad \rightarrow \quad 2\ I^- + 3\ O_2 \quad (3)$$

From the results of the color reaction, the amount of I$^-$ ions after photocatalysis was estimated to be 29 μmol in the solution (Figure S3). This value is consistent with the expected stoichiometric amount for O$_2$ evolution (43 μmol). These results thus indicate that O$_2$ is produced solely from photocatalyzed water oxidation reactions.

Metal oxide complexes containing Pb^{2+} cations, such as PbMoO$_4$ (BG: 3.3 eV),[6] RbPb$_2$Nb$_3$O$_{10}$ (BG: 2.6 eV),[7] and PbBi$_2$Nb$_2$O$_9$ (BG: 2.9 eV),[11] possess shallower valence bands due to mixing between the Pb6s and O2p orbitals. Accordingly, we were interested in PbCrO$_4$ for its electronic structure. Figure 3 shows the valence band X-ray photoelectron spectroscopy (valence XPS) data of PbCrO$_4$, TiO$_2$, and WO$_3$. The horizontal axes of these spectra were corrected by C1s (284.5 eV). It was found that the top valence band position of PbCrO$_4$ is more negative compared to that of WO$_3$ and TiO$_2$, which both possess a valence band consisting of the O2p orbital. Results from density functional theory (DFT) calculations using the structural parameters from PDF 98-002-4607 (Figure S4) also indicate that the valence band structure of PbCrO$_4$ is formed by hybridization of the O2p and Pb6s orbitals.

Next, we estimated the flat band potential of PbCrO$_4$ using a Mott-Schottky plot. Figure 4 depicts the Mott-Schottky plot of the PbCrO$_4$ electrode prepared by the squeegee method. From this result, the flat band potential of PbCrO$_4$ was estimated to be +0.03
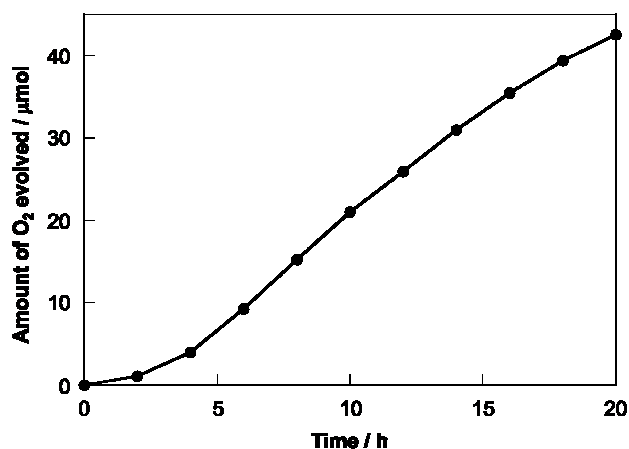
Figure 2 Reaction time course of water oxidation in the presence of IO$_3^-$ ion. Catalyst (10 mg), reactant solution (2 mM NaIO$_3$), light source (300 W Xe arc-lamp attached to L42 cut-off filter).
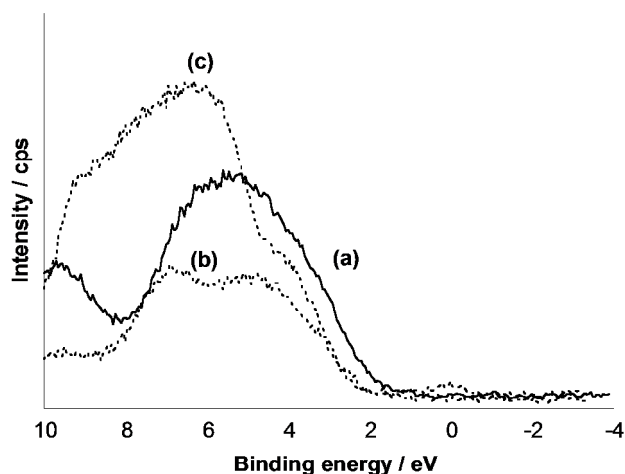
Figure 3 Valence band XPS data of (a) PbCrO$_4$, (b) TiO$_2$, and (c) WO$_3$. The horizontal axes of these spectra were corrected by C1s (284.5 eV).
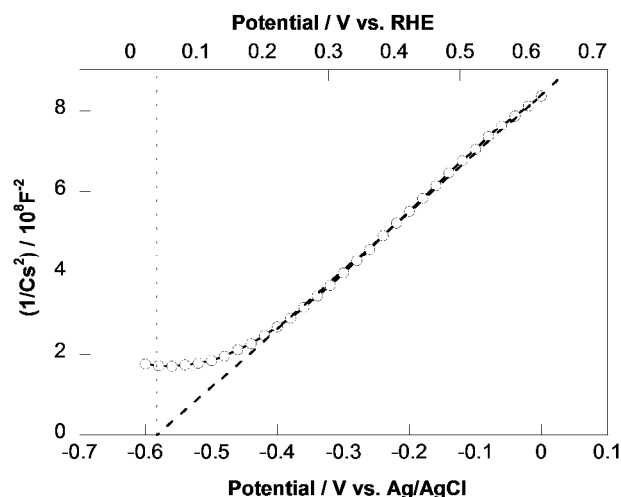
Figure 4 Mott-Schottky plot of PbCrO$_4$ electrode prepared by the squeegee method. Electrolyte: aqueous 1M phosphate buffer solution (pH 7). Periodicity: 965 Hz.

eV vs. RHE. It has been reported that the potential differences between conduction band minimum and flat band potential for n-type semiconductors (Ta$_2$O$_5$, TaON, and Ta$_3$N$_5$) are estimated to be ca. 0.3 eV.[15] Therefore, it is surmised that the conduction band minimum of PbCrO$_4$ is ca. -0.3–0 eV vs. RHE, if the potential difference is less than 0.3 eV.

From the results of diffuse reflection spectrum (DRS), valence XPS, Mott-Schottky plot, and DFT studies, the band structure of PbCrO$_4$ was elucidated as shown in Figure 5. The top of valence band potential of PbCrO$_4$, which consists of the O2p and Pb6s hybrid orbitals, can be estimated from the band gap and flat band potential values; this results in an estimated valence band potential of + 2.3 V vs. RHE. Consequently, PbCrO$_4$ was found to possess an attractive electronic structure to photocatalytically induce water oxidation (O$_2$/H$_2$O = +1.23 V). Recently, the electronically similar metal oxide complex BiVO$_4$ (BG: 2.4 eV) which also possesses shallow valence band consisting of Bi6s and O2p hybrid orbitals has attracted increasing attention as a visible light-induced water oxidation photocatalyst and photoelectrode. It is worth noting that
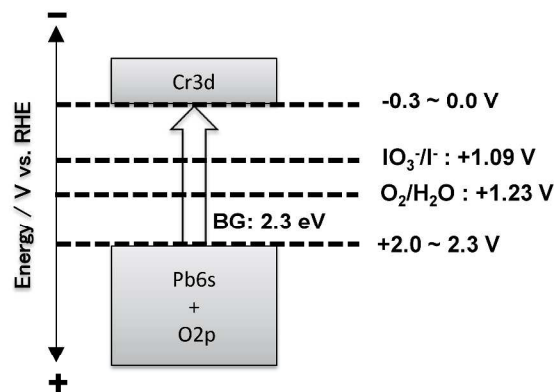
Figure 5 Band structure of PbCrO$_4$

the band gap of PbCrO$_4$ is narrower than that of BiVO$_4$. Therefore, this material is considered to be a promising photocatalyst and photoelectrode for water oxidation.

Conclusions

We successfully determined that Pt-metal loaded PbCrO$_4$ serves as a new oxide photocatalyst for water oxidation reactions under a wide spectrum of visible light. The results from this study demonstrate that O$_2$ evolution over Pt/PbCrO$_4$ proceeds photocatalytically, based on the quantified amounts of both the oxidation and reduction products (O$_2$ and I$^-$, respectively). From the results of DRS, valence XPS, Mott-Schottky plot, and DFT studies, we conclude that PbCrO$_4$ possesses an attractive electronic structure to photocatalytically promote water oxidation reactions with a redox mediator.

Acknowledgements

Notes and references

Energy Technology Research Institute, National Institute of Advanced Industrial Science and Technology (AIST), Central 5, 1-1-1 Higashi, Tsukuba, Ibaraki, 305-8565, Japan. E-mail: yugo-miseki@aist.go.jp, k.sayama@aist.go.jp.

† Electronic supplementary information (ESI) available: Fig. S1 to S3 are given. See DOI: 10.1039/c4ee01777c.

1 A. Kudo and Y. Miseki, *Chem. Soc. Rev.*, 2009, **38**, 253.

2 K. Sayama, K. Mukasa, R. Abe, Y. Abe and H. Arakawa, *Chem. Commun.*, 2001, 2416.

3 R. Abe, *Bull. Chem. Soc. Jpn.*, 2011, **84**, 1000.

4 K. Maeda, *ACS Catal.*, 2013, **3**, 1486.

5 Y. Miseki, H. Kusama, H. Sugihara and K. Sayama, *J. Phys. Chem. Lett.*, 2010, **1**, 1196.

6 A. Kudo, M. Steinberg, A. J. Bard, A. Campion, M. A. Fox, T. E. Mallouk, S. E. Webber and J. M. White, *Catal. Lett.*, 1990, **5**, 61.

7 J. Yoshimura, Y. Ebina, J. Kondo, K. Domen and A. Tanaka, *J. Phys. Chem.*, 1993, **97**, 1970.

8 A. Kudo and S. Hijii, *Chem. Lett.*, 1999, **28**, 1103.

9   A. Kudo, K. Omori and H. Kato, *J. Am. Chem. Soc.*, 1999, **121**, 11459.

10 H. Kato, H. Kobayashi and A. Kudo, *J. Phys. Chem. B*, 2002, **106**, 12441.

11 H. G. Kim and D. W. Hwang, J. S. Lee, *J. Am. Chem. Soc.*, 2004, **126**, 8912.

12 Y. Hosogi, K. Tanabe, H. Kato, H. Kobayashi and A. Kudo, *Chem. Lett.*, 2004, **33**, 28.

13 E. Bandiello, D. Errandonea, D. Martinez-Garcia, D. Santamaria-Perez, F. J. Manjón, *Phys. Rev. B*, 2012, **85**, 024108.

14 B. Cheng, H. Guo, J. Yu and X. Zhao, *J. Alloys Comp.*, 2007, **431**, L4.

15 W. J. Chun, A. Ishikawa, H. Fujisawa, T. Takata, J. N. Kondo, M. Hara, M. Kawai, Y. Matsumoto, K. Domen, *J. Phys. Chem. B*, 2003, **107**, 1798.